Sphingosine-1-Phosphate Protects Proliferating Endothelial Cells from Ceramide-Induced Apoptosis but not from DNA Damage–Induced Mitotic Death

Stéphanie Bonnaud,[1] Colin Niaudet,[1] Géraldine Pottier,[2] Marie-Hélène Gaugler,[1,3] Julie Millour,[1] Jacques Barbet,[1] Laure Sabatier,[2] and François Paris[1]

[1]Département de Recherche en Cancérologie, Institut National de la Santé et de la Recherche Médicale U601; Université de Nantes, Faculté des Sciences, Nantes, France; [2]CEA-DSV/DRR/LRO, Laboratoire de Radiobiologie et Oncologie; and [3]Institut de Radioprotection et de Sureté Nucléaire, DRPH/SRBE/LRPAT, Fontenay-aux-roses, France

Abstract

Because of the central role of the endothelium in tissue homeostasis, protecting the vasculature from radiation-induced death is a major concern in tissue radioprotection. Premitotic apoptosis and mitotic death are two prevalent cell death pathways induced by ionizing radiation. Endothelial cells undergo apoptosis after radiation through generation of the sphingolipid ceramide. However, if mitotic death is known as the established radiation-induced death pathway for cycling eukaryotic cells, direct involvement of mitotic death in proliferating endothelial radiosensitivity has not been clearly shown. In this study, we proved that proliferating human microvascular endothelial cells (HMEC-1) undergo two waves of death after exposure to 15 Gy radiation: an early premitotic apoptosis dependent on ceramide generation and a delayed DNA damage–induced mitotic death. The fact that sphingosine-1-phosphate (S1P), a ceramide antagonist, protects HMEC-1 only from membrane-dependent apoptosis but not from DNA damage–induced mitotic death proves the independence of the two pathways. Furthermore, adding nocodazole, a mitotic inhibitor, to S1P affected both cell death mechanisms and fully prevented radiation-induced death. If our results fit with the standard model in which S1P signaling inhibits ceramide-mediated apoptosis induced by antitumor treatments, such as radiotherapy, they exclude, for the first time, a significant role of S1P-induced molecular survival pathway against mitotic death. Discrimination between ceramide-mediated apoptosis and DNA damage–induced mitotic death may give the opportunity to define a new class of radioprotectors for normal tissues in which quiescent endothelium represents the most sensitive target, while excluding malignant tumor containing proproliferating angiogenic endothelial cells that are sensitive to mitotic death. [Cancer Res 2007;67(4):1803–11]

Introduction

For decades, DNA damage was considered as the principal cause of cell death induced by ionizing radiation. DNA double-strand breaks, which generate chromosomal aberrations, induce mitotic death (e.g., clonogenic or reproductive death). Mitotic death is a slow process occurring after a variable number of cell cycles (1), characterized by anaphase bridges, exclusion of micronuclei from the nucleus (2), cell enlargement (3), and generation of polyploid cells (4). Besides mitotic death, DNA damage is also involved in radiation-induced apoptosis by initiating signalization pathways that lead to the subsequent induction of a wide range of genes, such as *ATM* (5) or *p53* (6). New developments showed that other cell compartments are also involved in radiosensitivity. Indeed, cell membrane also represents a major target in radiation-induced apoptosis (7). Activation of the acid sphingomyelinase enzyme pool on the outer cell membrane layer potentiates sphingomyelin hydrolysis to ceramide, inducing membrane rearrangement, raft formation, and apoptotic signal transduction (8).

By supplying nutriments and oxygen, the endothelium network maintains tissue homeostasis. Vasculature represents a highly differentiated tissue where endothelial cells are quiescent in most of the normal physiologic conditions, except during tissue repair. Endothelium dysfunctions, such as loss of nonproliferating status during tumor angiogenesis, are involved in severe pathologies (9). Because of these physiologic outputs, understanding the death mechanism of the endothelial cell has a genuine relevance. *In vitro* radiosensitivity of endothelial cell has been essentially studied by clonogenic assays (10, 11). If clonogenic assay measures the capacity of the irradiated cell to divide into colony, correlation between clonogenic assay and mortality is partial. Indeed, clonogenic assay is related as much to survival and proliferation as to death, without discriminating the different types of death. New developments in radiobiology, such as generation of transgenic murine models, allowed to better define factors involved in endothelial cell radiosensitivity. *In vitro* (12) and *in vivo* (13) studies showed the crucial roles of acid sphingomyelinase enzyme activation and a rapid ceramide generation in radiation-induced endothelial cell death. Ionizing radiation acts directly on bovine aortic endothelial cell membrane preparations devoid of nuclei, proving that ceramide generation after irradiation is independent of DNA damage and cell cycle regulation induced by DNA double-strand breaks (14). Furthermore, invalidation of *acid sphingomyelinase* (*asmase*) gene in mice inhibited the radiation-induced endothelial cell apoptosis (15), which leads to tissue response as injury to the central nervous system (16), gastrointestinal syndrome (13), or blood-brain barrier disruption (17). Microvascular apoptosis has also been characterized by tumor response to high-dose radiotherapy. A 15 Gy irradiation of fibrosarcoma or melanoma tumor cells transplanted in mice rapidly induced a massive endothelial cell apoptosis via acid sphingomyelinase activation, which led to tumor regression (18). These results showed the importance of the acid sphingomyelinase and ceramide pair in endothelial cell apoptosis in normal or tumor tissue

Requests for reprints: François Paris, Institut National de la Sante et de la Recherche Medicale U601, Institut de Biologie, 9 quai Moncousu, 44093 Nantes cedex 01, France. Phone: 33-2-40-08-47-33; Fax: 33-2-40-35-66-97; E-mail: fparis@nantes.inserm.fr.

doi:10.1158/0008-5472.CAN-06-2802

integrity after ionizing radiation, as well as the critical role of endothelial cell in maintenance of normal or tumor integrity. Pharmacologic alteration of the ceramide metabolic pathway should modulate endothelial cell death and tissue response.

Sphingosine-1-phosphate (S1P), a ceramide metabolite, is a bioactive sphingolipid that has been characterized as a potent signal transduction–inducing molecule that exerts diverse biological responses, such as cellular differentiation, hypertrophy, proliferation, migration (19), and cell survival (20). S1P protection mechanisms seem to occur when apoptosis is dependent on ceramide generation (21). Indeed, S1P was shown to protect human umbilical vein endothelial cell (HUVEC) from C_2-ceramide–mediated apoptosis (22). *In vivo* studies using C57Bl/6 mouse model showed that S1P pretreatment in ovarian bursa protects mice from chemotherapy- or radiotherapy-induced sterility through inhibition of ceramide-mediated apoptosis in oocytes (23, 24). Ceramide/S1P balance has the capacity to modulate cell apoptosis and tissue radiosensitivity. However, no study has validated the potential protecting effect of S1P on endothelial cells after high-dose radiation.

If previous studies showed that quiescent endothelial cells, found in normal tissue, died by ceramide generation–dependent apoptosis after exposure to high dose of radiation (13, 17, 25, 26), the death mechanisms have not been explored for proliferating endothelial cells, which are present in pathologic tissues such as tumor angiogenesis. In this study, we propose to investigate the contribution of two major death pathways (i.e., DNA damage–induced mitotic death and ceramide generation–induced apoptosis) involved in radiosensitivity status of the proliferating endothelial cell. Because of its radioprotective effects in several cell models toward a large spectrum of stresses, the involvement of S1P in protecting proliferating endothelial cells will be more specifically studied in these two major radiosensitive pathways.

Materials and Methods

Cell Culture and Treatments

Human microvascular endothelial cells (HMEC-1) were kindly provided by F.J. Candal (Center for Disease Control, Atlanta, GA; ref. 27). HMEC-1 cells were seeded at a density of 20,000/cm^2 and allowed to reach subconfluence for 5 days in MCDB 131 medium (Invitrogen, Cergy Pontoise, France) supplemented with 15% FCS, 10 ng/mL epidermal growth factor, 2 μg/mL hydrocortisone, 2 mmol/L L-glutamine, 100 units/mL penicillin, and 100 μg/mL streptomycin, referred to as endothelial cell complete medium.

Irradiations of subconfluent HMEC-1 cells were carried out in a Faxitron CP160 irradiator (Faxitron X-ray Corporation, Buffalo Grove, IL) at a dose rate of 1.48 Gy/min and a total dose between 2 and 30 Gy. Two hours before irradiation, cell medium was changed to low-serum medium (MCDB 131 medium supplemented with 0.1% FCS, 2 μg/mL hydrocortisone, 2 mmol/L L-glutamine, 100 units/mL penicillin, and 100 μg/mL streptomycin). Different pharmacologic drugs were added to the low-serum medium 2 h before irradiation: 1 μmol/L fumonisin B1 (Biomol, Philadelphia, PA) or 1 μmol/L S1P (Biomol; prepared as previously described in ref. 23). Exceptions were made for desipramine (50 μmol/L; Sigma-Aldrich, St. Quentin-Favier, France), which was added 15 min before irradiation and removed 1 h after, and nocodazole (0.1 μg/mL; Sigma-Aldrich), which was added 24 h after radiation for another 24 h.

Detection of Apoptosis

Cell counting assay. As previously described (28), apoptotic fraction was calculated by taking the ratio of floating cell number to total cell number (floating + adherent). Floating cell population represented the nonadherent cells in the culture medium, and loosely adherent cells were derived from two PBS washes of the monolayer. Adherent cells were trypsinized. Cell number of both fractions was determined using Malassez slides.

Detection of apoptotic marker Apo2.7. Apo2.7 (7A6 antigen) has been described as a mitochondrial marker of apoptosis (29). Adherent and floating cells, either pooled or not, were washed twice with PBS, and labeled with the monoclonal antibody (mAb) anti–Apo2.7-phycoerythrin (clone 2.7A6A3) according to the supplier's recommendations (Immunotech, Marseilles, France). Acquisitions were done on a FACSCalibur flow cytometer (BD Biosciences, Le Pont de Claix, France), and data were analyzed using CellQuest software (BD Biosciences).

Cell Cycle Analysis

[^{3}H]thymidine incorporation. Sixteen hours after irradiation, HMEC-1 cells were incubated with low-serum medium containing [^{3}H]thymidine (1 μCi/mL) for 8 h. Cells were then trypsinized and harvested with a Titertek cell harvester (Flow Laboratories, Rickmansworth, United Kingdom) on glass fiber filter (Wallac Perkin-Elmer, Courtaboeuf, France). Cells were then dried and incubated with Betaplate scintillation liquid (Wallac Perkin-Elmer). β Radioactivity was counted by using a scintillation spectrometer (Wallac Perkin-Elmer). [^{3}H]thymidine incorporation was analyzed with the Microbeta Windows Workstation software (Wallac Perkin-Elmer).

Propidium iodide staining. Floating and adherent cells were pooled, washed with PBS, fixed in 70% ethanol for 20 min at −20°C, and stained with 40 μg/mL propidium iodide (Sigma-Aldrich) and 100 μg/mL RNase (Qiagen, Courtaboeuf, France) for 30 min at 37°C in the dark. Cell cycle phases were quantified using Flow Jo software (Tree Star, Ashland, OR).

DNA Damage Assessment

Detection of phosphorylated histone H2AX. For the detection of DNA double-strand breaks after irradiation, staining for phosphorylated H2AX (γH2AX) was conducted as described previously (30). Cells were trypsinized, washed with PBS, and fixed in 70% ethanol overnight at −20°C. Cells were rehydrated for 10 min in PBS/4% FCS/0.1% Triton X-100, and resuspended in 200 μL of mouse mAb against γH2AX (clone JBW301; Euromedex, Mundolsheim, France; 1:500 dilution in PBS/2% FCS/0.1% Triton X-100) for 2 h at room temperature. Cells were washed in PBS/2% FCS/0.1% Triton X-100 and resuspended in secondary antibody, a phycoerythrin-conjugated goat anti-mouse IgG F(ab′)$_2$ fragment (Beckman Coulter, Roissy, France; 1:100 dilution in PBS/2% FCS/0.1% Triton X-100) for 1 h at room temperature. Cells were washed and resuspended in 20 μg/mL 7-amino-actinomycin D (Sigma-Aldrich) before analysis with a BD FACSArray Bioanalyser (BD Biosciences). Analyses of flow cytometry data were conducted using CellQuest software.

Cytogenetic analyses. Twenty-two hours 30 min after 15 Gy irradiation, colchicine (0.1 μg/mL; Sigma-Aldrich) was added for 1 h 30 min before collecting the cells. Then, cultures were trypsinized and suspended in hypotonic solution (0.075 mol/L KCl), incubated for 20 min at 37°C, and fixed in methanol/acetic acid (3:1). Cell suspensions were dropped on slides and dried. Slides were processed according to the fluorochrome plus Giemsa method by Perry and Wolff (31) to score mitotic index (percentage of metaphase), chromosomal aberrations, and number of cell divisions done posttreatment. Cell culture duration postirradiation was determined to score chromosomal aberrations exclusively from the first division. Telomeres were detected by a (C3TA2)3PNA-Cy3 probe (Perceptive Biosystem, Boston, MA), whereas centromeres were detected by a Pan-centromere probe (Cambio, Cambridge, United Kingdom). Hybridized metaphases were captured with a charge coupled device camera (Zeiss, Jena, Germany) coupled to a Zeiss Axioplan microscope and were processed with the ISIS software (MetaSystems, Altlussheim, Germany). At least 100 metaphases were examined for each sample. We scored chromosome rearrangements, such as dicentrics or multicentrics, rings, and excess acentrics (i.e., we did not score the acentric generated with one dicentric chromosome). To determine the number of breaks per metaphase, the number of breaks per type of aberration was assigned as follows: one dicentric (two breaks), one tricentric (four breaks), one quadricentric (six breaks), one pentacentric (eight breaks), one ring (two breaks), and one minute or one acentric (one break).

Detection of micronuclei. Floating and adherent cells were pooled 48 h after 15 Gy irradiation, washed with PBS, spread on slides with a Cytospin (Thermo Electron Corp., Waltham, MA) at 800 rpm for 2 min, fixed in paraformaldehyde (0.5%) for 30 min, and permeabilized with Triton X-100 (0.1% in PBS) for 10 min. Slides were washed twice with PBS, incubated in 5 μg/mL propidium iodide (Sigma-Aldrich) and 1 mg/mL RNase (Qiagen) for 1 h at 37°C in the dark, and rinsed in 10 mmol/L Tris. Cells were visualized with a ×400 lens on a fluorescent microscope (Axiovert 200-M; Carl Zeiss, Göttingen, Germany).

Statistical Analysis

All values were reported as mean ± SD or SE as indicated. Data were analyzed using the Student's *t* test or the Mann-Whitney test (SIGMASTAT software, Jandel Scientific, Erkrath, Germany). Differences were considered as significant at $P < 0.05$ unless indicated otherwise.

Results

Irradiation induces endothelial cell apoptosis in a dose- and time-dependent manner. Exposure of subconfluent HMEC-1 to X-rays results in a dose- and time-dependent decrease in the number of adherent cells and increase in the number of floating cells. Twenty-four hours after radiation, 38.3 ± 4.9%, 48.6 ± 12.2%, and 75.2 ± 4.9% less adherent cells were quantified, respectively, in 5, 15, or 30 Gy irradiated cells compared with unirradiated cells. Floating cells in the culture medium increased with dose. Compared with control, 2-, 4.5-, and 6.5-fold higher floating cells were quantified in 5, 15, or 30 Gy conditions, respectively (Fig. 1*A*). The single dose of 15 Gy is chosen for the rest of the study because of the physiologic relevance of endothelial cell apoptosis after irradiation at high dose (13). The use of the apoptotic mitochondrial marker Apo2.7 confirms the induction of apoptotic cells after radiation (23.8% apoptotic cells 24 h after 15 Gy versus 8.4% for control; Fig. 1*B*). Furthermore, the fact that 90.2% of the floating cells are Apo2.7 positive validated our cell counting assay as an apoptotic assay (Fig. 1*B*). Similar to the dose-dependent quantification of endothelial cell death, we follow the generation of apoptotic HMEC-1 cells as a function of time. After a single 15 Gy

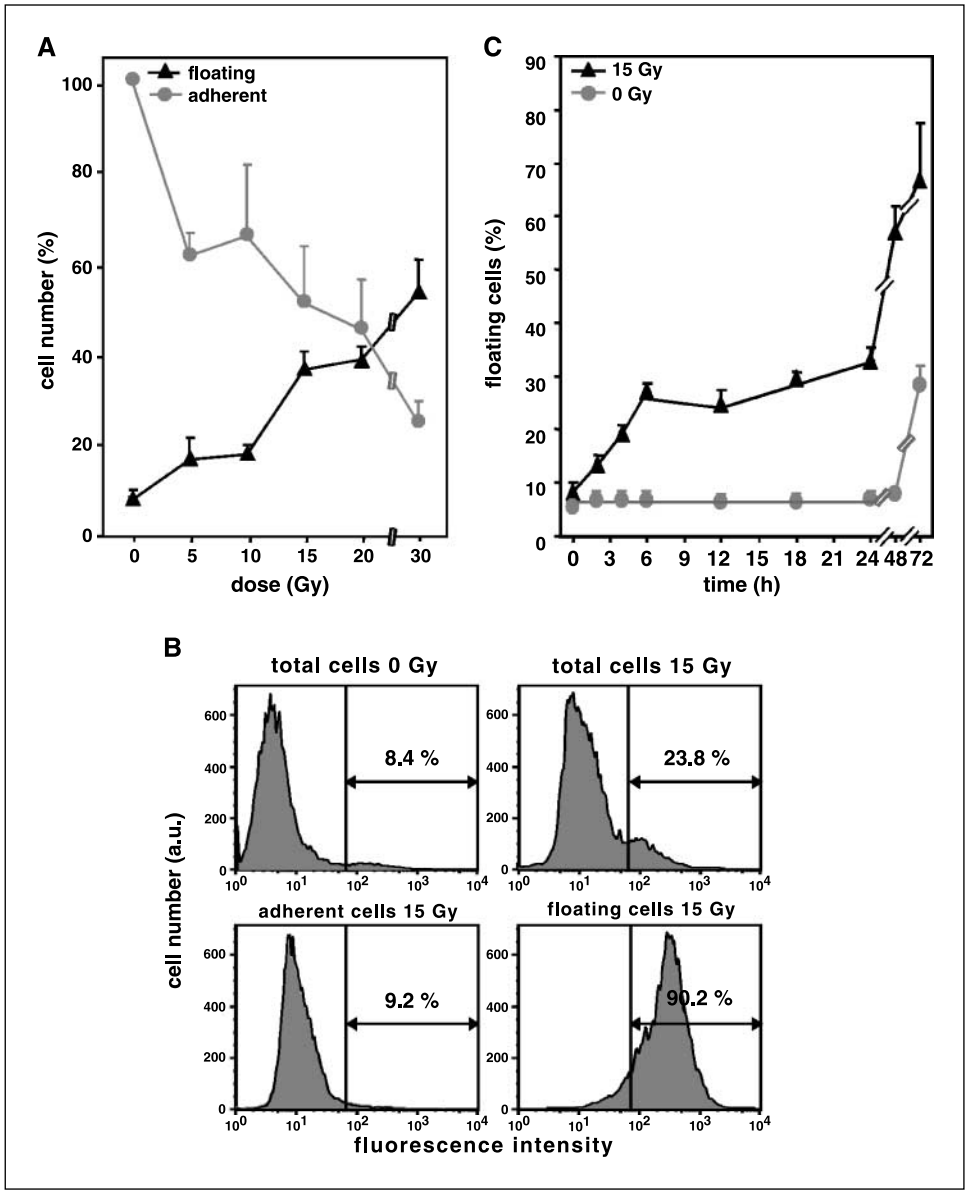

Figure 1. Irradiation induces endothelial cell apoptosis *in vitro* in a dose- and time-dependent manner. *A,* floating (▲) and adherent (●) cell number counts from subconfluent HMEC-1 24 h after exposure to 0, 5, 10, 15, 20, and 30 Gy. *Y-axis,* % [floating cells / (floating cells + adherent cells)] at each dose for the floating cell curve and % [(adherent cells at *x* Gy) / (adherent cells at 0 Gy)] for the adherent cell curve. *Points,* mean from at least three independent experiments; *bars,* SE. *B,* determination of apoptotic cell death done by flow cytometry using apoptotic marker Apo2.7 24 h after 15 Gy irradiation. Original data from one of three experiments. *C,* apoptotic cell counting assay of unirradiated (●) and irradiated (▲) HMEC-1 incubated 0, 2, 4, 6, 12, 18, 24, 48, and 72 h after 15 Gy radiation exposure. Values are mean ± SD from three to eight independent experiments ($P < 0.001$).

irradiation, two waves of floating cells were observed: the first one reached a plateau at 25% of apoptotic cells 6 h postradiation until 24 h; the second one started 24 h postradiation increasing to 66 ± 20.2% of floating cells at 72 h (Fig. 1*C*) and reaching a peak of >86% at 92 h (data not shown).

Inhibition of ceramide pathway by S1P or desipramine blocks early apoptosis but not late death. To confirm that radiation-induced apoptosis in HMEC-1 cells is mediated by acid sphingomyelinase activation–induced ceramide generation, as shown in endothelial cells *in vivo* in the central nervous system (16) or in gastrointestinal syndrome (13), experiments were carried out using the acid sphingomyelinase inhibitor desipramine. Apoptotic counting assay done 24 h postirradiation shows that 50 μmol/L desipramine pretreatment significantly decreased apoptosis by 52.4%, compared with the 15 Gy control (P = 0.003), to background level of nonirradiated cells (Fig. 2*A*). Nevertheless, desipramine treatment does not inhibit the late apoptosis observed at 72 h during the second wave of death (39.4 ± 1.4% of apoptosis for control and 42.5 ± 1.4% for desipramine-treated cells; P > 0.1). Besides the acid sphingomyelinase pathway, *de novo* biosynthesis by ceramide synthase represents another major ceramide generation pathway activated in endothelial cells after radiation (26, 32). To evaluate the specificity of the acid sphingomyelinase pathway, the ceramide synthase inhibitor fumonisin B1 was used. We observed no difference between radiation-induced apoptosis of 1 μmol/L fumonisin B1–treated HMEC-1 and untreated cells, 24 and

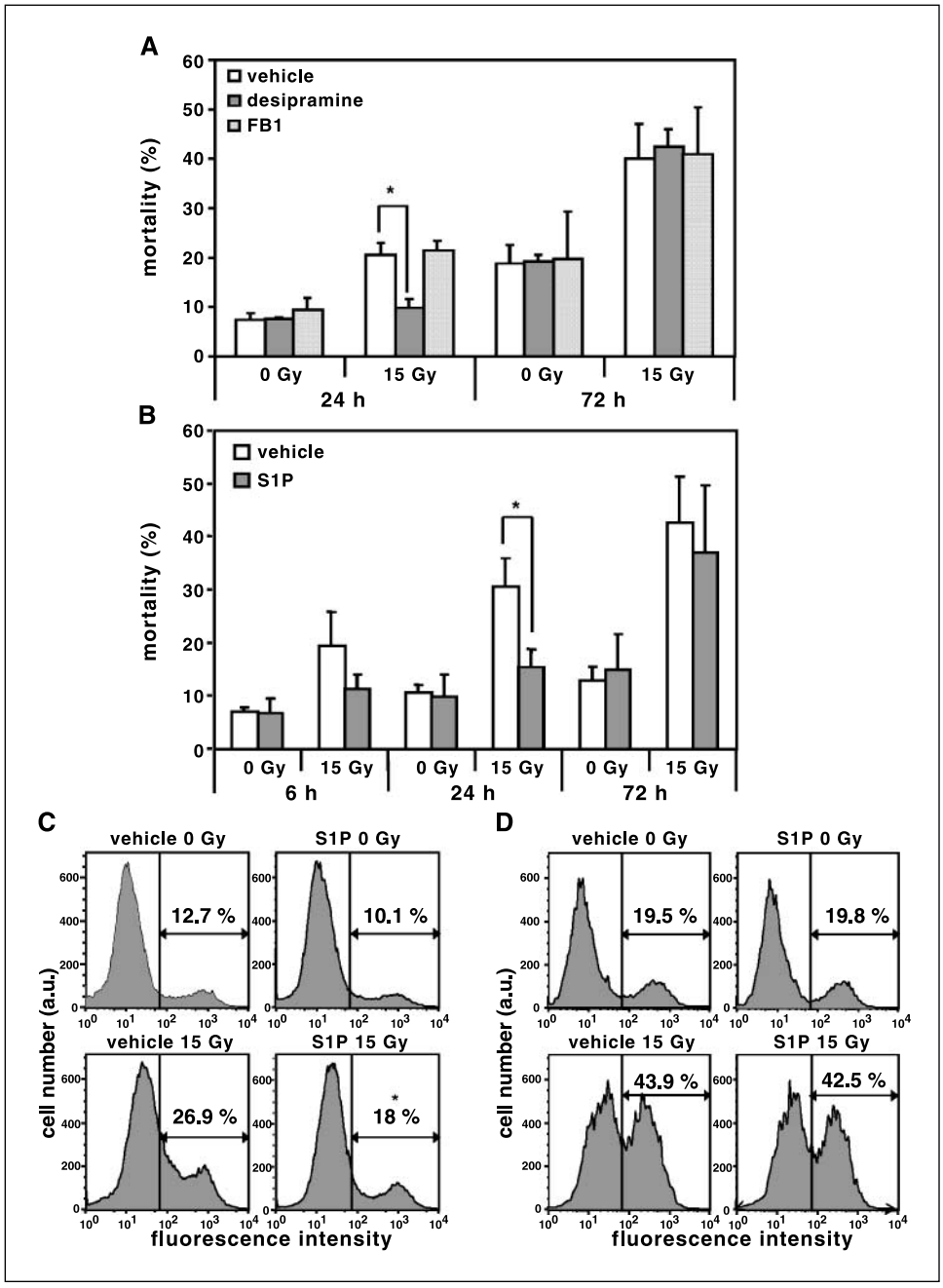

Figure 2. Inhibition of ceramide pathway by S1P blocks early apoptosis but not late death. *A,* comparison of apoptotic cell counting assay of HMEC-1 24 h after exposure to 15 Gy radiation treated either with 50 μmol/L desipramine (*filled columns*), 1 μmol/L fumonisin B1 treatment (*shaded columns*), or control (*empty columns*). *Columns,* mean from two independent experiments carried out in triplicate; *bars,* SD (P < 0.005). *B,* apoptotic cell counting of 1 μmol/L S1P-pretreated (*filled columns*) or vehicle-pretreated (*empty columns*) HMEC-1 incubated for 6, 24, and 72 h after exposure to 15 Gy radiation. *Columns,* mean from three independent experiments; *bars,* SD (P < 0.05). *C* and *D,* determination of apoptotic cell death done by flow cytometry using the apoptotic marker Apo2.7 of 15 Gy irradiated HMEC-1 incubated 24 h (*C*) or 72 h (*D*). Values are mean ± SE from three independent experiments done in duplicate ($P \leq 0.001$). Original FACS data from one of three experiments.

72 h after 15 Gy irradiation (Fig. 2*A*), proving the major role of the acid sphingomyelinase and ceramide pair in HMEC-1 early radiosensitivity.

Because of the ceramide/S1P rheostat model, we investigated if S1P could protect HMEC-1 from radiation-induced apoptosis mediated by ceramide generation. Two hours of pretreatment with 1 μmol/L S1P lowered the number of apoptotic cells by 2-fold, 24 h after 15 Gy, nearly to the background level (30.5 ± 5.2% of apoptosis for control and 15.3 ± 3.4% for S1P-treated cells, $P = 0.013$; Fig. 2*B*). Apo2.7 staining (Fig. 2*C*) and terminal deoxynucleotidyl transferase–mediated nick end labeling (TUNEL) assay (data not shown) confirmed S1P radioprotection, which pointed out a significant 33.3% and 21.2% decrease in apoptotic HMEC-1 cell percentage in 15 Gy irradiated condition pretreated with 1 μmol/L S1P compared with the 15 Gy control, respectively. The specificity of the S1P radioprotection was determined by dihydro-S1P, a sphingolipid related to S1P. Indeed, 2 h of 1 μmol/L dihydro-S1P pretreatment does not inhibit the HMEC-1 apoptosis rate 24 h after 15 Gy (data not shown).

Although S1P inhibits radiation-induced apoptosis in HMEC-1 cells 24 h after radiation, protection by S1P is not effective in the late death wave. Indeed, no statistical difference in floating cell counting assay was found 72 h after 15 Gy irradiation between the S1P-treated and untreated conditions (36.9 ± 12.8% for S1P-treated group versus 42.7 ± 8.5% for vehicle-treated group; $P > 0.5$; Fig. 2*B*). Results are confirmed by Apo2.7 staining (Fig. 2*D*). After exposure to 15 Gy radiation, we observed percentages of death of 43.9% for control and 42.5% for S1P-pretreated cells.

S1P does not protect HMEC-1 from DNA damage and mitotic catastrophe. The fact that desipramine or S1P has no action on late death shows that the second wave of death is independent of acid sphingomyelinase activation–induced ceramide generation and membrane signaling. DNA damage–induced cell death is also a major cell death pathway after X-ray radiation (33). Cells containing γH2AX foci (each focus represents a single DNA double-strand break) were quantified by fluorescence-activated cell sorting (FACS) analysis as a function of time, irradiation, and S1P treatment. Maximum γH2AX-positive cell ratio was observed within the window between 30 min and 1 h after exposure to 15 Gy radiation (83.2 ± 6.7% in sham condition versus 74.3 ± 11.2% in S1P condition 30 min postradiation, $P > 0.5$; Fig. 3*A*). Furthermore, no difference in the mean of fluorescence intensity, representing the number of foci per cell, was observed at the different time points of the experiment (data not shown). Similar kinetic profiles of DNA double-strand break induction and their repair, represented by the increase and the decrease of γH2AX-positive cells, respectively, were observed in HMEC-1 cells treated or not by S1P (Fig. 3*A*).

Irradiation-induced DNA double-strand breaks leads to chromosomal rearrangements, mitotic catastrophe, and death. Radiation-induced chromosomal damage, quantified by the number of chromosomal breaks per metaphase, was studied 24 h after exposure to radiation. Because of the high level of cell death and low level of metaphases observed after exposure to 15 Gy radiation, chromosomal breaks per metaphase were analyzed in HMEC-1 cells irradiated at 0, 2, and 5 Gy. First, we observed that the percentage of breaks per metaphase increased in a dose-dependent manner, independent of treatment with S1P or its vehicle (0 Gy, $P = 0.5$; 2 Gy, $P > 0.3$; 5 Gy, $P > 0.5$; Fig. 3*B*). Furthermore, no difference in quality of breaks, such as multicentric, acentric, and minute chromosomal damages, was observed in irradiated

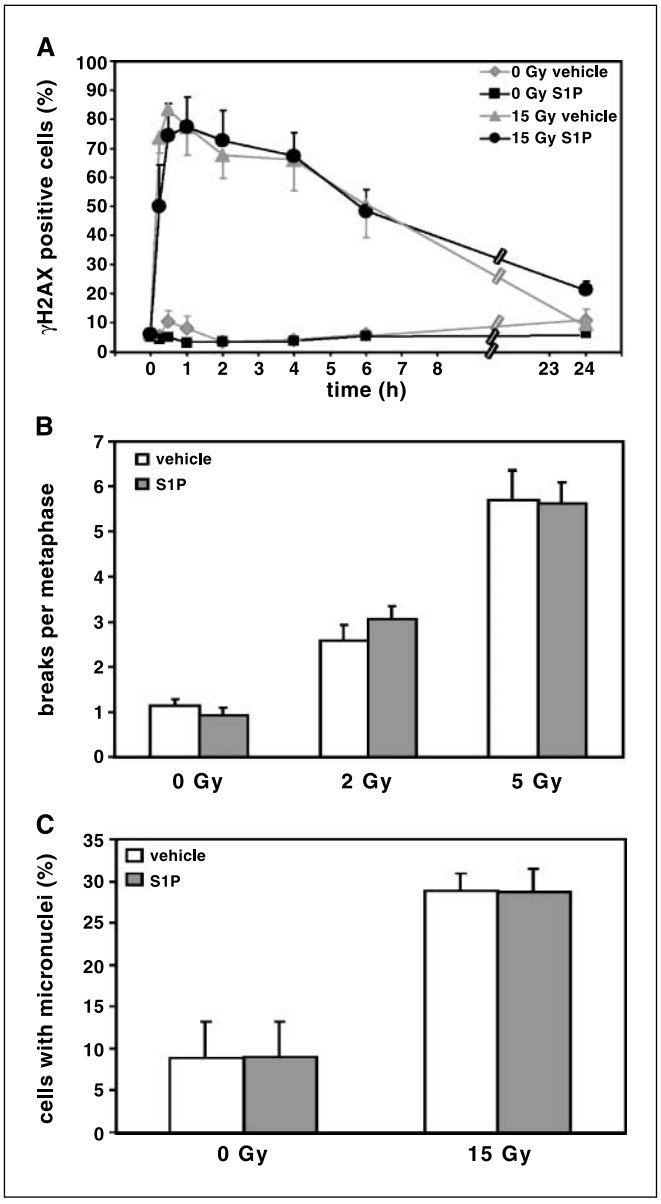

Figure 3. S1P does not protect HMEC-1 from DNA damage and mitotic catastrophe. *A,* labeling for DNA damage foci with mAb against γH2AX of HMEC-1 treated with 1 μmol/L S1P (●) or vehicle (▲) before exposure to 15 Gy radiation. Labeling occurs 0, 15, or 30 min, and 1, 2, 4, 6, or 24 h postradiation. *Points,* mean from four independent experiments done in duplicate or triplicate; *bars,* SE. *B,* chromosomal breaks of 1 μmol/L S1P-pretreated (*filled columns*) or vehicle-pretreated (*empty columns*) HMEC-1 in metaphase by colchicine treatment exposed 24 h after 15 Gy radiation exposure. *Columns,* mean of 100 metaphases analyzed per condition; *bars,* SE. *C,* micronuclei formation of 1 μmol/L S1P-pretreated or vehicle-pretreated HMEC-1 exposed 48 h after 15 Gy radiation exposure. *Columns,* mean from four independent experiments with 200 nuclei per experiment; *bars,* SD.

condition with or without S1P incubation (data not shown). Experiments carried out at 10 and 15 Gy irradiation showed the same rate and types of breaks per metaphase tendencies when HMEC-1 cells were treated with S1P or its vehicle (data not shown; metaphase number is too small for statistical distribution).

Severe chromosomal damage fails to produce correct chromosomal segregation after mitosis, which results in micronuclei exclusion and leads to mitotic death (1). To assess the mechanism

of death during the second-wave postirradiation, micronuclei formation was quantified 48 h after exposure to 15 Gy radiation. A 3.3-fold increase of cells with one or more micronuclei was observed after radiation compared with nonirradiated cells, proving that the late death represents cells that are dying by mitotic death (Fig. 3*C*). Furthermore, pretreatment with S1P does not inhibit the amount of cells with one or more micronuclei after irradiation [S1P + 15 Gy treatment (28.8 ± 2.1%) versus 15 Gy treatment (28.7 ± 2.7%); $P > 0.9$; Fig. 3*C*].

S1P does not modulate cell cycle inhibition involved in mitotic death. Mitotic death is considered to be a slow process occurring after a variable number of cell cycles (34). To confirm the nonprotective effect of S1P during the mitotic death wave, proliferation and regulation of cell cycle were studied after radiation. First, we ensured that S1P radioprotection into the first wave of apoptotic death is not due to an upsurge of endothelial cell proliferation using [^{3}H]thymidine incorporation assay. In nonirradiated HMEC-1 cells, 24 h after S1P treatment, proliferation increased by 1.2-fold compared with untreated cells, confirming the proangiogenic action of S1P (Fig. 4*A*; ref. 35). However, after 15 Gy irradiation, cell proliferation decreased by 7.3- and 8.9-fold for sham- and S1P-treated cells, respectively, but no difference between vehicle or S1P-treated cell proliferation was observed ($P > 0.8$; Fig. 4*A*). Results were confirmed by analysis of mitotic index. Twenty-four hours after a dose range of 2 to 15 Gy, HMEC-1 mitotic index decreased in a dose-dependent manner. No statistical difference between S1P-treated cell mitotic index and control was observed (for 15 Gy, $P > 0.7$; Fig. 4*B*).

Cell cycle distribution 24 h after 15 Gy irradiation was examined by propidium iodide incorporation (Fig. 4*C*). Unirradiated cultures maintained a typical cell cycle distribution of asynchronous populations (G_1, 41 ± 6.8% for control and 43.4 ± 4.6% for S1P; S, 15.8 ± 8% for control and 18.4 ± 6.1% for S1P; G_2-M, 23.1 ± 11.2% for control and 19.6 ± 4.8% for S1P). As already been shown, irradiation-induced G_2-M arrest was observed in HMEC-1 since 6 h postirradiation. Moreover, S1P does not modulate the efficiency or the kinetic of the G_2-M cell cycle control after irradiation. Twenty-four hours after exposure to 15 Gy radiation, 48.2 ± 8.2% of the control cells were arrested in G_2-M versus 50 ± 5.5% for S1P-treated cells (Fig. 4*C*; $P > 0.6$).

Combination of S1P and nocodazole treatments highly protects proliferating endothelial cell by inhibiting ceramide apoptotic pathway and mitotic death, respectively. Because cell cycle has to be processed to develop mitotic death, we used nocodazole, which inhibits microtubule formation, to block or delay mitotic death. Forty-eight hours after 15 Gy irradiation, 30.6% decreased cell death was observed in nocodazole-treated HMEC-1 compared with control cells (Fig. 5*A*). S1P treatment showed no significant difference between S1P or sham-treated irradiated cells, thus confirming data shown in Fig. 2*B* and *D* ($P > 0.2$; Fig. 5*A*). To further validate that HMEC-1 radiation-induced death involves two different mechanisms (e.g., ceramide-mediated apoptosis and DNA damage–mediated mitotic death), HMEC-1 were treated with S1P before irradiation and with nocodazole after irradiation. Enhancements of radioprotection by 2- and 1.5-fold were observed when 15 Gy irradiated HMEC-1 cells were treated by S1P + nocodazole ($P \leq 0.001$) and by nocodazole alone ($P \leq 0.001$; Fig. 5*A*), respectively.

Because of their involvement in mitotic death, micronuclei incidence was determined in irradiated HMEC-1 to validate the protection by dual S1P + nocodazole treatments (Fig. 5*B*). First, as expected, treatment by S1P did not modify the incidence of micronuclei in irradiated HMEC-1 ($P > 0.9$; Fig. 5*B*). Moreover, cell population irradiated and treated with nocodazole contains 40.5% fewer cells with micronuclei compared with control ($P = 0.004$; Fig. 5*B*). Better radioprotection was observed when cells were treated with S1P and nocodazole together. In this condition, incidence of cells with micronuclei decreased to 37.5% compared with untreated cells ($P \leq 0.001$; Fig. 5*B*).

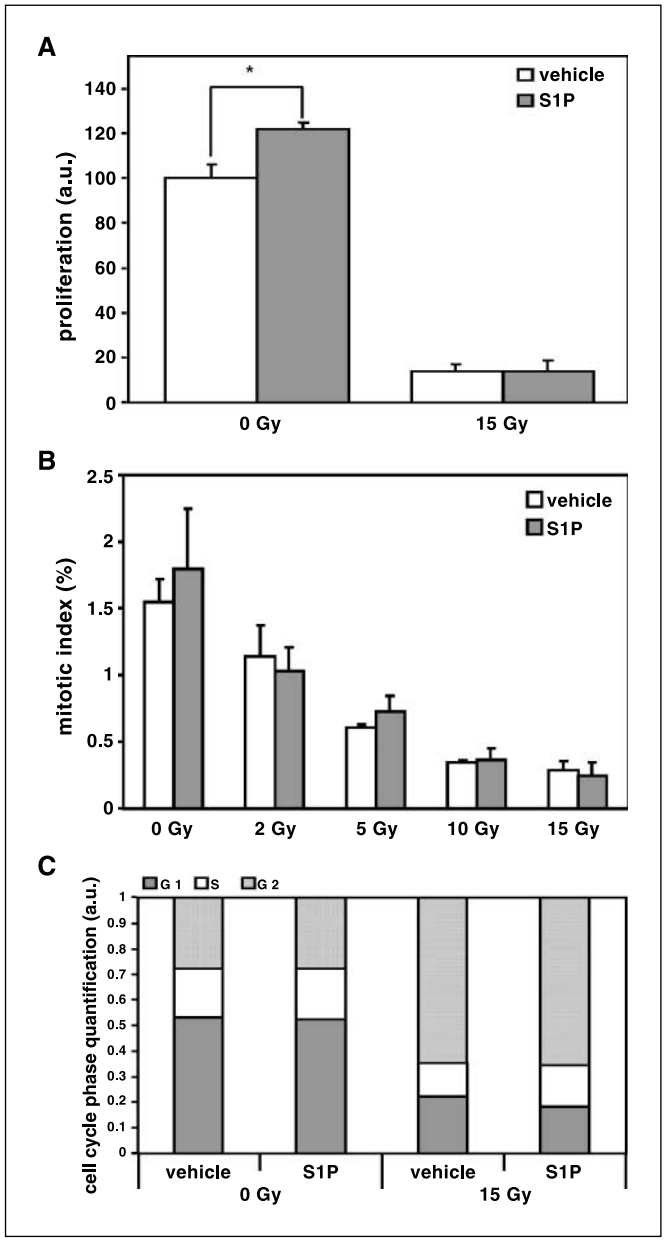

Figure 4. S1P does not modify cell cycle inhibition involved in mitotic catastrophe. *A,* S1P-treated (*filled columns*) and vehicle-treated (*empty columns*) HMEC-1 proliferation 24 h after 15 Gy irradiation done using [^{3}H]thymidine incorporation. *Columns,* mean from five independent experiments; *bars,* SD. *B,* mitotic index of S1P pretreatment (*filled columns*) or sham control cells (*empty columns*) HMEC-1 after 0, 2, 5, 10, and 15 Gy irradiation. *Columns,* mean from three independent experiments with 1,000 nuclei per experiment; *bars,* SD. *C,* cell cycle analysis using Flow Jo software after propidium iodide staining. *Columns,* mean from four independent experiments done in duplicate.

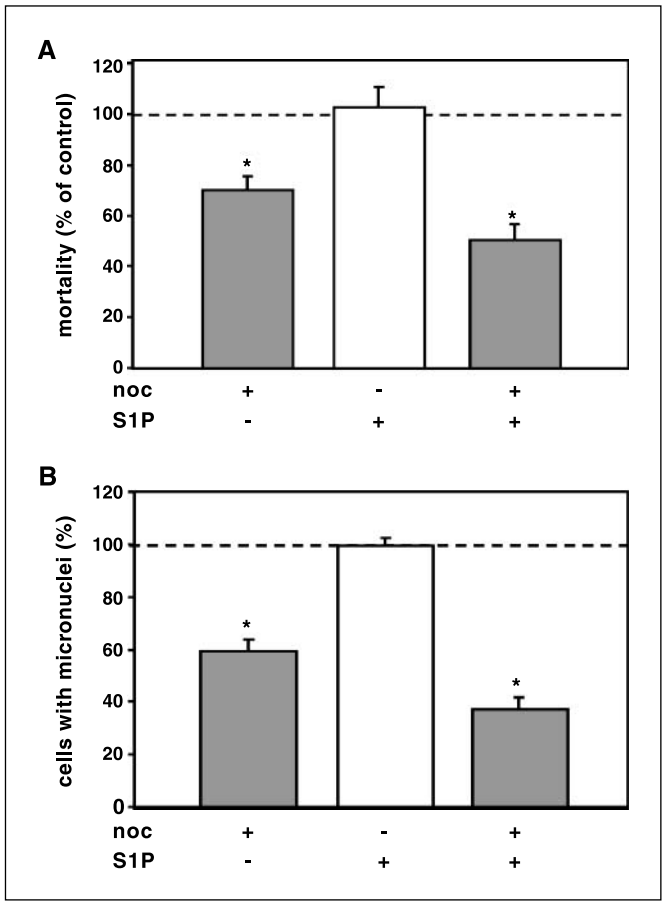

Figure 5. Arrest of ceramide pathway by S1P and mitotic catastrophe by nocodazole inhibit radiation-induced endothelial cell death. *A,* 15 Gy irradiated HMEC-1 treated 2 h before irradiation with 1 μmol/L S1P and 24 h postradiation with 0.1 μg/mL nocodazole, and stained 48 h postradiation with apoptotic marker Apo2.7. *Columns,* mean from four independent experiments done in duplicate or triplicate; *bars,* SE. *B,* micronuclei formation after 48 h of 15 Gy irradiated HMEC-1 treated 2 h before irradiation with 1 μmol/L S1P and 24 h postradiation with 0.1 μg/mL nocodazole. *Columns,* mean from four independent experiments with 200 nuclei per experiment; *bars,* SD.

Discussion

The effect of endothelial cell radiosensitivity in tissue damage and tumor regression to high-dose radiation has been previously described (13, 18, 36). Confluent endothelial cells have been shown to die after radiation through generation of proapoptotic factor ceramide (14). However, if mitotic death represents the established radiation-induced death pathway for most dividing eukaryotic cells, involvement of mitotic death in proliferating endothelial cell radiosensitivity has not been distinctly shown. In this study, we prove that proliferating endothelial cells undergo mitotic death if ceramide-mediated death is inhibited by S1P (Fig. 6).

Apoptotic cell count, Apo2.7 staining, and TUNEL assay of irradiated HMEC-1 cells showed that HMEC-1 radiosensitivity comprises two waves of death. The first wave of death, between 0 and 24 h postradiation, depended on acid sphingomyelinase activation and ceramide generation because desipramine treatment was able to inhibit this early endothelial death. The second wave of death occurring 24 h after radiation was insensitive to desipramine treatment and thus independent of acid sphingomyelinase/ceramide apoptotic pathway (Fig. 6). Chromosomal aberration studies and micronuclei assays correlated the second wave of death with DNA damage generation and mitotic death, the definitive involvement of which was proven by inhibition of late cell death by nocodazole, a mitosis inhibitor.

DNA damage triggers molecular pathways controlled by key molecular node, especially ceramide synthase and p53. In bovine aortic endothelial cells, fumonisin B1 blocked X-ray–induced death through inhibition of ceramide synthase, making it an attractive target to explain our late cell death phenomenon (32). In our endothelial cell model, maximum tolerated dose of fumonisin B1 was not able to inhibit the second wave of death, meaning that ceramide synthase activation does not seem to be involved in radiation-induced HMEC-1 mitotic death. The major discrepancy between Liao's study and ours is the proliferation status of the endothelial cells. X-ray experiments in bovine aortic endothelial cells have been realized using quiescent endothelial cells, excluding the mitotic death analysis, whereas our experiments allowed use of proliferating HMEC-1 cells to study the involvement of mitotic death and its molecular factors in endothelial cell radiosensitivity.

HMEC-1 cells are immortalized with SV40 large T-antigen, which inactivates p53 and might modify DNA damage–induced apoptosis and cell cycle arrest. However, previous results have shown that acid sphingomyelinase– and ceramide-mediated apoptosis induced in microvascular endothelium was independent of p53 status. At the difference of invalidation of *asmase* gene, disruption of p53 in mice neither modified high-dose radiation–induced endothelial cell apoptosis inside the lamina propria and around the crypt nor inhibited small intestine necrosis or animal death timing (13). Our first wave of death in HMEC-1 is dependent on acid sphingomyelinase activation and ceramide generation, in which SV40 is not known to be interfering with. Mitotic death occurs after cell cycle G_2 arrest. If p53 is known to regulate cell cycle after ionizing

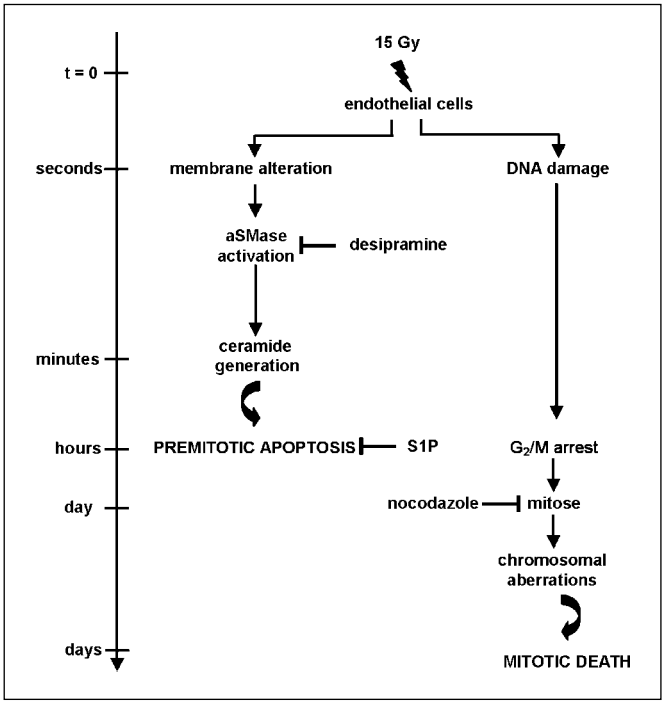

Figure 6. Schematic sequence of molecular events leading to ceramide-mediated premitotic apoptosis and DNA damage–induced mitotic death.

radiation, especially by inducing G_1 arrest through increase of p21 expression, different studies also showed that X-ray–induced apoptosis occurring after G_2 arrest might be independent of p53 (37–39). We ultimately prove the relevance of the two waves of death by confirming data obtained in the SV40-immortalized endothelial cell, in human primary macrovascular endothelial cells. Indeed, S1P is able to protect human primary macrovascular endothelial cells from the first wave of radiation toxicity at 24 h but not from the second wave of death observed at 72 h (data not shown), as shown in HMEC-1. Further studies will help to better understand the molecular pathways involved in the second wave of death.

Pretreatment of HMEC-1 with a therapeutic relevant dose of S1P protects against early apoptosis, which is dependent on ceramide generation induced by radiation exposure, but not the late death, which is dependent on DNA damage. Moreover, S1P action in irradiated HMEC-1 cells seems specific, because other sphingolipids, such as dihydro-S1P, do not enhance radioprotection (data not shown). A key function of S1P is to mediate vascular growth by enhancing endothelial cell proliferation. This proproliferative action of S1P could explain its radioprotective activity. This survival mechanism has already been embodied by lovastatin, a lipid-lowering molecule, which inhibits HUVEC radiosensitivity at late time point after radiation, partially by an increase of endothelial cell proliferation (40). Our results using [^{3}H]thymidine incorporation or mitotic index analysis showed that S1P does not protect microvascular endothelial cell by an upsurge of proliferation (Fig. 4*A* and *B*). Apo2.7 apoptotic staining definitely proves direct inhibition of ceramide-mediated apoptosis by S1P treatment (Fig. 2*C*). Our results fit with the main dogma of the "ceramide/S1P rheostat," which determines the death and survival status of cells exposed to lethal stress (41). Moreover, our study is the first one to show the pharmacologic input of S1P in modulation of microvascular endothelial cell apoptosis after exposure to a high dose of ionizing radiation.

To understand the absence of S1P protection toward mitotic death, we wondered if S1P interfered with DNA damage–controlled pathway. We first studied the rate of loss of γH2AX, a phosphorylated histone localized in a DNA repair foci (42). The fact that S1P- or vehicle-treated cells throughout expressed a similar percentage of cells with foci and a similar average number of foci per cell (mean value) proves that S1P pretreatment does not affect the rate of DNA double-strand breaks induced by ionizing radiation and does not confer an enhancement of repair machinery. Because insufficiently repaired or misrepaired double-strand breaks might lead to chromosome breaks, deletions, and translocations (43), we also analyzed the percentage of breaks per metaphase with respect to the ionizing radiation dose. S1P pretreatment did not modulate the rate of breaks by metaphase (quantitative analysis) or the types of breaks, such as ring, acentric, and multicentric (qualitative analysis), induced by increasing dose of ionizing radiation (Fig. 3*B*; and data not shown).

Chromosomal abnormalities, appearance of micronuclei, and cell cycle modulation, which we all validated in our endothelial cell model, are the main characteristic events of mitotic death (1). Furthermore, mitotic death requires a transient G_2-M arrest and also takes a longer incubation period (>24 h) until execution of cell death compared with premitotic apoptosis (39). As previously shown by Khodarev et al. (11), we also observed by propidium iodide staining the strong G_2-M arrest and the dead cells in sub-G_1 phase 48 h postradiation, characteristic of the mitotic death. Mitotic death was thought to be exhibited mainly by non-hematopoietic cell lineages, although the involvement of mitotic death in proliferating endothelial cell radiosensitivity has not been clearly shown, except when endothelial cells are irradiated after angiostatin pretreatment (10).

Modulating the early ceramide-dependent death by S1P and the late DNA damage–dependent death by nocodazole affected proliferating endothelial cell death after radiation and showed the independence of the two waves of death. Compared with sham-irradiated cells, S1P pretreatment does not reduce the amount of cells with micronuclei, a mitotic death marker, explaining the high level of mitotic death observed 48 h postradiation in both conditions. Differences in late death and micronuclei rates (Fig. 5*A* and *B*, respectively) between nocodazole-treated and S1P + nocodazole–treated irradiated cells are explained by the fact that S1P and nocodazole treatment gives an additive protection, whereas nocodazole treatment prevents or delays endothelial cell only from late death. Other studies already showed that S1P protects cells from genotoxic agents (21, 23, 24, 44). However, none of these studies were able to discriminate protection due to inhibition of ceramide-mediated apoptosis from the one dependent on DNA damage radiosensitivity. Our extensive study on proliferating endothelial cell death after radiation represents the first study to exclude S1P radioprotection from the process involving interaction with DNA repair machinery or cell cycle modulation.

As recently pointed out (45), S1P metabolism has taken center stage in cancer development and treatment. High expression of sphingosine kinase 1, an enzyme transforming sphingosine to S1P, in tumor cell was correlated with low patient survival (46). Treatment of nude mice by sphingosine kinase 1 inhibitors reduced gastric and mammary adenocarcinoma tumor growth (47). Neutralizing by mAb, the pathophysiologic S1P secreted by cancer cells and platelets in the serum delayed the growth of the tumor by preventing angiogenesis (48). Thus, chronic secretion of S1P appears to play a major role in tumorigenesis by protecting tumor cells and by enhancing microvascularization induced by other key proangiogenic growth factors [vascular endothelial growth factor and basic fibroblast growth factor (bFGF); ref. 45]. These protumoral sides of S1P are counterbalanced by the fact that S1P radioprotection, at a therapeutic, single, relevant low dose, is specific on ceramide-dependent endothelial cell apoptosis. This offers a promising approach for pharmacologically improving the radioprotection of normal tissues. Indeed, adult normal tissue vasculature is quiescent (49) because of the equilibrium between angiogenic promoters and inhibitors (9). Because of this non-proliferative status of endothelial cells, DNA damage–induced mitotic death cannot be the main observable type of death, explaining why endothelial cells died exclusively by the acid sphingomyelinase/ceramide–mediated apoptosis: acid sphingomyelinase knockout mice have an endothelium resistant to ionizing radiation in brain, lung, and intestine tissues compared with wild-type mice or knockout mice for DNA damage–sensing factors, such as DNA-PK, ATM, or p53 (13, 16, 26). Like bFGF injection, S1P treatment should modulate ceramide in endothelial cells *in vivo* and protect normal tissues from radiation-induced toxicity. However, pathologic endothelial cells have the capacity to divide (9). This proliferating status opens the door to mitotic death, which S1P is not able to block. All of these important biological issues warrant more intensive future *in vivo* investigation. Mitotic death induced by radiotherapies and most of the chemotherapies are developed to target essentially cells with high proliferating

capacity. Our data prove that S1P radioprotection is only due to inhibition of acid sphingomyelinase/ceramide–mediated apoptosis. In this circumstance, S1P protection will not be ubiquitous: Therefore, selective protection by S1P of early apoptosis but not mitotic death may give the opportunity to define a selective radioprotector for normal tissues, in which quiescent endothelial cells represent the most sensitive target, but not tumor containing endothelial cells with high proliferating characteristics, which will be sensitive to mitotic death.

Acknowledgments

Received 7/28/2006; revised 10/13/2006; accepted 12/10/2006.

Grant support: Commission of the European Communities, Association Contract FI6R-CT-2003-508842 RISC-RAD, and ACI «jeunes chercheuses-jeunes chercheurs». S. Bonnaud's Ph.D. fellowship was assumed by Association pour la Recherche sur le Cancer and a grant of Region Pays de la Loire and CEA.

The costs of publication of this article were defrayed in part by the payment of page charges. This article must therefore be hereby marked *advertisement* in accordance with 18 U.S.C. Section 1734 solely to indicate this fact.

We thank Dr. I. Corre for critical review of the manuscript.

References

1. Roninson IB, Broude EV, Chang BD. If not apoptosis, then what? Treatment-induced senescence and mitotic catastrophe in tumor cells. Drug Resist Updat 2001;4:303–13.
2. Dewey WC, Ling CC, Meyn RE. Radiation-induced apoptosis: relevance to radiotherapy. Int J Radiat Oncol Biol Phys 1995;33:781–96.
3. Lock RB, Ross WE. Possible role for p34cdc2 kinase in etoposide-induced cell death of Chinese hamster ovary cells. Cancer Res 1990;50:3767–71.
4. Muller WU, Nusse M, Miller BM, Slavotinek A, Viaggi S, Streffer C. Micronuclei: a biological indicator of radiation damage. Mutat Res 1996;366:163–9.
5. Cortez D, Guntuku S, Qin J, Elledge SJ. ATR and ATRIP: partners in checkpoint signaling. Science 2001;294:1713–6.
6. Sancar A, Lindsey-Boltz LA, Unsal-Kacmaz K, Linn S. Molecular mechanisms of mammalian DNA repair and the DNA damage checkpoints. Annu Rev Biochem 2004;73:39–85.
7. Hannun YA. Functions of ceramide in coordinating cellular responses to stress. Science 1996;274:1855–9.
8. Gulbins E, Li PL. Physiological and pathophysiological aspects of ceramide. Am J Physiol Regul Integr Comp Physiol 2006;290:R11–26.
9. Carmeliet P. Angiogenesis in life, disease and medicine. Nature 2005;438:932–6.
10. Hari D, Beckett MA, Sukhatme VP, et al. Angiostatin induces mitotic cell death of proliferating endothelial cells. Mol Cell Biol Res Commun 2000;3:277–82.
11. Khodarev NN, Kataoka Y, Murley JS, Weichselbaum RR, Grdina DJ. Interaction of amifostine and ionizing radiation on transcriptional patterns of apoptotic genes expressed in human microvascular endothelial cells (HMEC). Int J Radiat Oncol Biol Phys 2004;60:553–3.
12. Haimovitz-Friedman A, Balaban N, McLoughlin M, et al. Protein kinase C mediates basic fibroblast growth factor protection of endothelial cells against radiation-induced apoptosis. Cancer Res 1994;54:2591–7.
13. Paris F, Fuks Z, Kang A, et al. Endothelial apoptosis as the primary lesion initiating intestinal radiation damage in mice. Science 2001;293:293–7.
14. Haimovitz-Friedman A, Kan CC, Ehleiter D, et al. Ionizing radiation acts on cellular membranes to generate ceramide and initiate apoptosis. J Exp Med 1994;180:525–5.
15. Santana P, Pena LA, Haimovitz-Friedman A, et al. Acid sphingomyelinase-deficient human lymphoblasts and mice are defective in radiation-induced apoptosis. Cell 1996;86:189–99.
16. Pena LA, Fuks Z, Kolesnick RN. Radiation-induced apoptosis of endothelial cells in the murine central nervous system: protection by fibroblast growth factor and sphingomyelinase deficiency. Cancer Res 2000;60:321–7.
17. Li YQ, Chen P, Haimovitz-Friedman A, Reilly RM, Wong CS. Endothelial apoptosis initiates acute blood-brain barrier disruption after ionizing radiation. Cancer Res 2003;63:5950–6.
18. Garcia-Barros M, Paris F, Cordon-Cardo C, et al. Tumor response to radiotherapy regulated by endothelial cell apoptosis. Science 2003;300:1155–9.
19. Hla T. Signaling and biological actions of sphingosine 1-phosphate. Pharmacol Res 2003;47:401–7.
20. Olivera A, Rosenfeldt HM, Bektas M, et al. Sphingosine kinase type 1 induces G12/13-mediated stress fiber formation, yet promotes growth and survival independent of G protein-coupled receptors. J Biol Chem 2003;278:46452–60.
21. Cuvillier O, Pirianov G, Kleuser B, et al. Suppression of ceramide-mediated programmed cell death by sphingosine-1-phosphate. Nature 1996;381:800–3.
22. Lee MJ, Thangada S, Claffey KP, et al. Vascular endothelial cell adherens junction assembly and morphogenesis induced by sphingosine-1-phosphate. Cell 1999;99:301–12.
23. Morita Y, Perez GI, Paris F, et al. Oocyte apoptosis is suppressed by disruption of the acid sphingomyelinase gene or by sphingosine-1-phosphate therapy. Nat Med 2000;6:1109–14.
24. Paris F, Perez GI, Fuks Z, et al. Sphingosine 1-phosphate preserves fertility in irradiated female mice without propagating genomic damage in offspring. Nat Med 2002;8:901–2.
25. Maj JG, Paris F, Haimovitz-Friedman A, Venkatraman E, Kolesnick R, Fuks Z. Microvascular function regulates intestinal crypt response to radiation. Cancer Res 2003;63:4338–41.
26. Ch'ang HJ, Maj JG, Paris F, et al. ATM regulates target switching to escalating doses of radiation in the intestines. Nat Med 2005;11:484–90.
27. Ades EW, Candal FJ, Swerlick RA, et al. HMEC-1: establishment of an immortalized human microvascular endothelial cell line. J Invest Dermatol 1992;99:683–90.
28. Lawrence TS, Davis MA, Hough A, Rehemtulla A. The role of apoptosis in 2′,2′-difluoro-2′-deoxycytidine (gemcitabine)-mediated radiosensitization. Clin Cancer Res 2001;7:314–9.
29. Zhang C, Ao Z, Seth A, Schlossman SF. A mitochondrial membrane protein defined by a novel monoclonal antibody is preferentially detected in apoptotic cells. J Immunol 1996;157:3980–7.
30. Sedelnikova OA, Rogakou EP, Panyutin IG, Bonner WM. Quantitative detection of (125)IdU-induced DNA double-strand breaks with γ-H2AX antibody. Radiat Res 2002;158:486–92.
31. Perry P, Wolff S. New Giemsa method for the differential staining of sister chromatids. Nature 1974;251:156–8.
32. Liao WC, Haimovitz-Friedman A, Persaud RS, et al. Ataxia telangiectasia-mutated gene product inhibits DNA damage-induced apoptosis via ceramide synthase. J Biol Chem 1999;274:17908–17.
33. Valerie K, Povirk LF. Regulation and mechanisms of mammalian double-strand break repair. Oncogene 2003;22:5792–812.
34. Ross GM. Induction of cell death by radiotherapy. Endocr Relat Cancer 1999;6:41–4.
35. Licht T, Tsirulnikov L, Reuveni H, Yarnitzky T, Ben-Sasson SA. Induction of pro-angiogenic signaling by a synthetic peptide derived from the second intracellular loop of S1P3 (EDG3). Blood 2003;102:2099–107.
36. Cho CH, Kammerer RA, Lee HJ, et al. Designed angiopoietin-1 variant, COMP-Ang1, protects against radiation-induced endothelial cell apoptosis. Proc Natl Acad Sci U S A 2004;101:5553–8.
37. Chang WP, Little JB. Delayed reproductive death in X-irradiated Chinese hamster ovary cells. Int J Radiat Biol 1991;60:483–96.
38. Iwamoto K, Shinomiya N, Mochizuki H. Different cell cycle mechanisms between UV-induced and X-ray-induced apoptosis in WiDr colorectal carcinoma cells. Apoptosis 1999;4:59–66.
39. Shinomiya N. New concepts in radiation-induced apoptosis: "premitotic apoptosis" and "postmitotic apoptosis". J Cell Mol Med 2001;5:240–53.
40. Nubel T, Damrot J, Roos WP, Kaina B, Fritz G. Lovastatin protects human endothelial cells from killing by ionizing radiation without impairing induction and repair of DNA double-strand breaks. Clin Cancer Res 2006;12:933–9.
41. Maceyka M, Payne SG, Milstien S, Spiegel S. Sphingosine kinase, sphingosine-1-phosphate, and apoptosis. Biochim Biophys Acta 2002;1585:193–201.
42. MacPhail SH, Banath JP, Yu TY, Chu EH, Lambur H, Olive PL. Expression of phosphorylated histone H2AX in cultured cell lines following exposure to X-rays. Int J Radiat Biol 2003;79:351–8.
43. Dasika GK, Lin SC, Zhao S, Sung P, Tomkinson A, Lee EY. DNA damage-induced cell cycle checkpoints and DNA strand break repair in development and tumorigenesis. Oncogene 1999;18:7883–99.
44. Otala M, Suomalainen L, Pentikainen MO, et al. Protection from radiation-induced male germ cell loss by sphingosine-1-phosphate. Biol Reprod 2004;70:759–67.
45. Milstien S, Spiegel S. Targeting sphingosine-1-phosphate: a novel avenue for cancer therapeutics. Cancer Cell 2006;9:148–50.
46. Van Brocklyn JR, Jackson CA, Pearl DK, Kotur MS, Snyder PJ, Prior TW. Sphingosine kinase-1 expression correlates with poor survival of patients with glioblastoma multiforme: roles of sphingosine kinase isoforms in growth of glioblastoma cell lines. J Neuropathol Exp Neurol 2005;64:695–705.
47. French KJ, Schrecengost RS, Lee BD, et al. Discovery and evaluation of inhibitors of human sphingosine kinase. Cancer Res 2003;63:5962–9.
48. Visentin B, Vekich JA, Sibbald BJ, et al. Validation of an anti-sphingosine-1-phosphate antibody as a potential therapeutic in reducing growth, invasion, and angiogenesis in multiple tumor lineages. Cancer Cell 2006;9:225–38.
49. Hobson B, Denekamp J. Endothelial proliferation in tumours and normal tissues: continuous labelling studies. Br J Cancer 1984;49:405–13.